Approximation Study Of Heat Transfer For Darcy-Forchheimer-Brinkman Model In Porous Cavity Confined Between Two Finite Thickness Walls

Ahmed M. Jumaa[#1], Ameer S. Dawood[#2] and Hekmat Sh. Mustafa[#3]

#1University of Mosul, College of Computer Sciences & Mathematics, Department of Mathematics, altaieahm@yahoo.com

#2University of Mosul,College of Engineering, Department of Mechanical Engineering, amirsd1954@yahoo.com

#3University of Mosul, College of Computer Sciences & Mathematics, Department of Mathematics, heksha@yahoo.com

ABSTRACT

Effects of a conductive wall on natural convection heat transfer in a rectangular enclosure filled with porous media sandwiched by two finite thickness walls is studied numerically in this article. The horizontal heating is considered, where the vertical walls heated isothermally at different temperatures while the horizontal walls are kept adiabatic.

The general flow model known as the Brinkman-Forchheimer-extended Darcy mode is used in the mathematical formulation for the porous layer and finite difference method is applied to solve the dimensionless governing equations. The governing parameters considered are the Rayleigh number ($10^3 \leq Ra \leq 10^6$), the wall to porous thermal conductivity ratio ($0.1 \leq Kr \leq 10$), the Darcy number ($10^{-6} \leq Da \leq 1$), the porosity of the porous region ($0.2 \leq \epsilon \leq 0.9$), and the ratio of wall thickness to its height ($0.25 \leq D \leq 0.375$).

The results are presented to show the effect of these parameters on the fluid flow and heat transfer characteristics.

Keywords:conjugate heat transfer, porous media, Brinkman-Forchheimer-extended Darcy model, finite difference method.

INTRODUCTION

The analysis of natural convection heat transfer in fluid saturated porous media plays an important role in many practical applications. These include geothermal engineering, thermal insulation systems, packed bed chemical reactors, porous heat exchangers, oil separation from sand by steam, underground disposal of nuclear waste materials, food storage, electronic device cooling, to name a few applications. Significant advances have been made in developing the momentum equation that governs the fluid flow in porous media, starting from Darcy's law to generalized model. A generalized model for the fluid flow through a porous medium was developed to account for inertial effects, boundary effects, and a variable porosity medium. These effects are incorporated by using the general flow model known as the Brinkman-Forchheimer-extended Darcy model. The literature concerning the experimental and numerical studies on convective flow in porous media is abundant and a comprehensive bibliography concerned with this topic can be found in the monographs and books by Vafai and Hadim [8], Ingham and Pop [3], Vafai [7], Nield and Bejan [2] and Vadasz [9]. Natural convection in finite porous enclosures has received considerable attention over the last several years and, in particular, non-Darcy effects on natural convection in porous media have received a great deal of attention recently [4]. Al-Amiri [1] considered the two insulated horizontal walls of finite thickness. Recently, Varol [10] and Saleh [6] analyzed convective flows of the Darcy-Benard convective in a thick bottom-walled enclosure. The present study is carried out to investigate the effects of a conductive wall on natural convection heat transfer in a rectangular enclosure filled with porous media sandwiched by two finite thickness walls and the effect of the main parameters on the fluid flow and heat transfer characteristics. The general flow model known as the Brinkman-Forchheimer-extended Darcy mode is used in the mathematical formulation for the porous layer.

NOMENCLATURE

x x-coordinate, (m) .
X non-dimensional X-coordinate .
Y y-coordinates, (m).
Y non-dimensional Y-coordinate.
u velocity component in x-direction, $(m.s^{-1})$.
U non-dimensional velocity component in X-direction.
v velocity component in y-direction, $(m.s^{-1})$.
V non-dimensional velocity component in Y-direction.
Ra Rayleigh number, $(g\beta(T_h - T_c)kH/\vartheta\alpha)$.
Pr Prandtl number, (ϑ/α) .
P non-dimensional pressure.
T dimensional temperature, (K).
k_p thermal conductivity of the porous, $(W.m^{-1}.k^{-1})$.
k_w thermal conductivity of the wall, $(W.m^{-1}.k^{-1})$.
kr thermal conductivity ratio, (k_w/k_p).
D the ratio of wall thickness to the height ($D=\frac{d}{H}$).
k the permeability of porous layer, (m^2).
H height of the cavity, (m) .
F_y body force, (N) .
Nu local Nusselt number.
$\overline{Nu}$ average Nusselt number.
g gravitational acceleration, $(m.s^{-2})$.
L length of the cavity , (m) .
d thickness of the solid walls,(m).
Da Darcy number, (k/H^2)
T time, (s).

Greek symbols

Ψ dimensionless stream function.
Ω dimensionless vorticity.
θ non-dimensional temperature .
α effective thermal diffusivity, $(m^2.s^{-1})$.
β coefficient of thermal expansion, (K^{-1}).
ϑ kinematic viscosity $(m^2.s^{-1})$.
ρ density, $(kg.m^3)$.
τ non-dimensional time.
ϵ the porosity of porous region.

Subscripts

c cold.
h hot.
f fluid part.
s solid part.
p porous layer.

2. MATHEMATICAL FORMULATION

2.1 Problem definition:

A natural convective flow and heat and mass transfers inside a vertical enclosure filled with a fluid saturated porous media sandwiched between two equal-thickness walls are considered and displayed in Figure 2.It is assumed that the left vertical wall of the cavity heated to the constant temperature Th and the right vertical wall cooled to the constant temperature T_c, where $T_h > T_c$, and the horizontal walls are adiabatic. The porous medium is assumed to be homogeneous and thermally isotropic. The saturated fluid within the medium is in a local thermodynamic equilibrium (LTE) with the solid matrix. The fluid flow is unsteady, laminar and incompressible. The pressure work and viscous dissipation are all assumed negligible.

The thermophysical properties of the porous medium are taken to be constant. However, the Boussinesq approximation takes into account of the effect of density variation on the buoyancy force, in which the fluid density is assumed constant except in the buoyancy term of the equation of motion. Furthermore, the solid matrix is made of spherical particles, while the porosity and permeability of the medium are assumed to be uniform throughout the rectangular cavity.

The Darcy-Forchheimer- Brinkman model was used to represent the fluid transport within the porous medium in the investigation of a convective flow through a cavity.

2.2 Governing Equations:

The generalized model for a natural convective flow and heat and mass transfers inside a vertical enclosure filled with a fluid saturated porous media sandwiched between two equal-thickness walls can be expressed by the following equations:

Continuity Equation

$$\frac{\partial u}{\partial x}+\frac{\partial v}{\partial y}=0 \quad \text{....}\ldots\ldots\ldots\ldots\ldots\ldots\ldots\ldots\ldots\ldots\ldots\ldots(1)$$

Momentum Equation (x-direction)

$$\frac{1}{\epsilon}\frac{\partial u}{\partial t}+\frac{1}{\epsilon^2}u\frac{\partial u}{\partial x}+\frac{1}{\epsilon^2}v\frac{\partial u}{\partial y}=-\frac{1}{\rho}\frac{\partial p}{\partial x}+\frac{\vartheta}{\epsilon}\left(\frac{\partial^2 u}{\partial x^2}+\frac{\partial^2 u}{\partial y^2}\right)-\left(F\frac{\rho}{\sqrt{K}}|\overline{W}|+\frac{\mu}{K}\right)u \quad \text{....(2)}$$

Momentum Equation (y-direction)

$$\frac{1}{\epsilon}\frac{\partial u}{\partial t}+\frac{1}{\epsilon^2}u\frac{\partial u}{\partial x}+\frac{1}{\epsilon^2}v\frac{\partial u}{\partial y}=-\frac{1}{\rho}\frac{\partial p}{\partial x}+\frac{\vartheta}{\epsilon}\left(\frac{\partial^2 u}{\partial x^2}+\frac{\partial^2 u}{\partial y^2}\right)-\left(F\frac{\rho}{\sqrt{K}}|\overline{W}|+\frac{\mu}{K}\right)u+F_y \quad \text{....(3)}$$

Energy Equation

$$\sigma\frac{\partial T_p}{\partial t}+u\frac{\partial T_p}{\partial x}+v\frac{\partial T_p}{\partial y}=\alpha\left(\frac{\partial^2 T_p}{\partial x^2}+\frac{\partial^2 T_p}{\partial y^2}\right) \quad \text{....(4)}$$

and the energy equation for the impermeable wall is:

$$\frac{\partial T_w}{\partial t}=\alpha\left(\frac{\partial^2 T_w}{\partial x^2}+\frac{\partial^2 T_w}{\partial y^2}\right) \quad \text{....(5)}$$

where: $\sigma=\frac{\left[\varepsilon(\rho c_p)_f+(1-\varepsilon)(\rho c_p)_s\right]}{(\rho c_p)_f}$, $|\overline{W}|=\sqrt{u^2+v^2}$

In equation (2), the last three terms are the Brinkman (or friction) term, the Darcy term and Forchheimer (or inertia) term. For a packed-sphere bed, the permeability (K) and the Forchheimer coefficient (F) are related to the porosity by:

$k=\frac{{d_p}^2\epsilon^3}{A(1-\epsilon^2)}$ and $F=\frac{B}{(150\,\epsilon^3)^{1/2}}$

where A and B are empirical constants: A=150 and B=1.75 . The physical meaning of the other quantities are mentioned in the Nomenclature.

The body force per unit mass due to buoyancy in the y-direction (F_y) can be obtained by the Boussinesq approximation:

$$\rho=\rho_0\left(1+\beta(T-T_c)\right) \quad \text{....(6)}$$

Where (β) is the volume coefficient of thermal expansion and (ρ_0) is the bulk fluid density .Thus, the body force (F_y) becomes:

$$F_y=g\beta(T-T_c) \quad \text{....(7)}$$

substituting the equation (7) in the equation (3), we have:

$$\frac{1}{\epsilon}\frac{\partial u}{\partial t}+\frac{1}{\epsilon^2}u\frac{\partial u}{\partial x}+\frac{1}{\epsilon^2}v\frac{\partial u}{\partial y}=-\frac{1}{\rho}\frac{\partial p}{\partial x}+\frac{\vartheta}{\epsilon}\left(\frac{\partial^2 u}{\partial x^2}+\frac{\partial^2 u}{\partial y^2}\right)-\left(F\frac{\rho}{\sqrt{K}}|\overline{W}|+\frac{\mu}{K}\right)u+g\beta\,(T-T_c) \quad \text{.....(8)}$$

In the present study, the heat capacity ratio σ is taken to be unity since the thermal properties of the solid matrix and the fluid are assumed identical.

The equations from (1) to (8) can be written in terms of the dimensionless stream function Ψ and vorticity Ω as follow:

$U=\frac{\partial \Psi}{\partial Y}$, $V=-\frac{\partial \Omega}{\partial X}$, $\Omega=\frac{\partial V}{\partial X}-\frac{\partial U}{\partial Y}$ together with the following non-dimensional variables:

$$X=\frac{x}{H},Y=\frac{y}{H},U=\frac{uH}{\alpha},V=\frac{vH}{\alpha},\tau=\frac{t\alpha}{H^2},P=\frac{pL^2}{\rho\alpha^2},\Psi=\frac{\psi}{\alpha},\Omega=\frac{\omega H^2}{\alpha},\theta=\frac{T-T_c}{T_h-T_c}$$

Thus, the dimensionless form of the governing equations can be written as:

$$\frac{\partial^2\Psi}{\partial X^2}+\frac{\partial^2\Psi}{\partial Y^2}=-\Omega \quad \text{....(9)}$$

$$\frac{\partial \theta_w}{\partial \tau} = \frac{\partial^2 \theta_w}{\partial X^2} + \frac{\partial^2 \theta_w}{\partial Y^2} \quad \text{.....(10)}$$

$$\frac{1}{\epsilon}\frac{\partial \Omega}{\partial \tau} + \frac{1}{\epsilon^2}\frac{\partial \Psi}{\partial Y}\frac{\partial \Omega}{\partial X} - \frac{1}{\epsilon^2}\frac{\partial \Psi}{\partial X}\frac{\partial \Omega}{\partial Y} = \frac{1}{\epsilon} Pr\left(\frac{\partial^2 \Omega}{\partial X^2} + \frac{\partial^2 \Omega}{\partial Y^2}\right) - \left(\frac{F}{\sqrt{Da}}|w| + \frac{Pr}{Da}\right)\Omega + Ra\, Pr \frac{\partial \theta_p}{\partial X} \quad \text{.....(11)}$$

$$\frac{\partial \theta_p}{\partial \tau} + \frac{\partial \Psi}{\partial Y}\frac{\partial \theta_p}{\partial X} - \frac{\partial \Psi}{\partial X}\frac{\partial \theta_p}{\partial Y} = \frac{\partial^2 \theta_p}{\partial X^2} + \frac{\partial^2 \theta_p}{\partial Y^2} \quad \text{.....(12)}$$

where: $\mathrm{Ra} = \frac{g\beta kH\,(T - T_c)}{\vartheta \alpha}$ is the Rayleigh number, $\mathrm{Pr} = \frac{\vartheta}{\alpha}$ is the Prandtl number and $\mathrm{Da} = \frac{k}{H^2}$ is the Darcy number.

2.3 Dimensionless Initial And Boundary Conditions:

Initial Condition

$for\ \tau = 0$:

$$\theta = \theta_w = \theta_p = \Psi = \Omega = 0 \quad \text{.....(13a)}$$

Boundary Condition

$for\ \tau > 0$:

$$\theta = 1 \ , \ \Psi = 0 \quad at \quad X = \frac{L}{H} \ , \ 0 < Y < 1 \quad \text{.....(13b)}$$

$$\theta = 0 \ , \ \Psi = 0 \quad at \quad X = \frac{L}{H} \ , \ 0 < Y < \frac{L}{H} \quad \text{.....(13c)}$$

$$\frac{\partial \theta}{\partial Y} = 0 \ , \ \Psi = 0 \ , \Omega = -\frac{\partial^2 \Psi}{\partial Y^2} \ \ at \ \ Y = 0 \ , 0 < X < \frac{L}{H} \quad \text{.....(13d)}$$

$$\frac{\partial \theta}{\partial Y} = 0 \ , \ \Psi = 0 \ , \Omega = -\frac{\partial^2 \Psi}{\partial Y^2} \ \ at \ \ Y = 1 \ , 0 < X < \frac{L}{H} \quad \text{.....(13e)}$$

$$\theta_p = \theta_w \ , \ \frac{\partial \theta_p}{\partial X} = Kr \frac{\partial \theta_w}{\partial X} \ , \Psi = 0 \ , \Omega = -\frac{\partial^2 \Psi}{\partial X^2} \ at \ X = D \ and \ X = \frac{L}{H} - D, 0 < Y < 1 \quad \text{.....(13f)}$$

where $\mathrm{Kr} = \frac{K_w}{K_p}$ is the thermal conductivity ratio. The physical quantities of interest in this problem are the local and average Nusselt numbers, defined respectively by:

$$Nu = -\left(\frac{\partial \theta}{\partial X}\right)_{X = D, \frac{L}{H} - D} \quad ; \quad \overline{Nu} = \int_0^1 Nu dy \quad \text{.....(14)}$$

3. NUMERICAL VALIDATION

The accuracy of the numerical code was validated by comparing the results with the published work of H.Saleh&I.Hashim [5] in the case of a porous enclosure with finite wall thickness as shown in Figure 1 . Table 1 shows that the average Nusselt number are in good agreement with the solutions reported by the leteratures.These comprehensive verification efforts demonstrated the robustness and accuracy of the present computation.

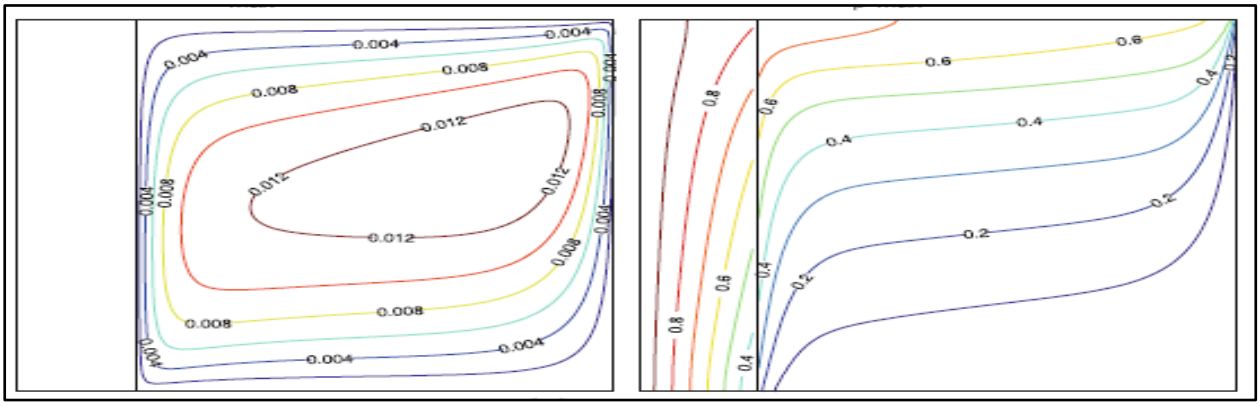

(a) |Ψ|=0.013275

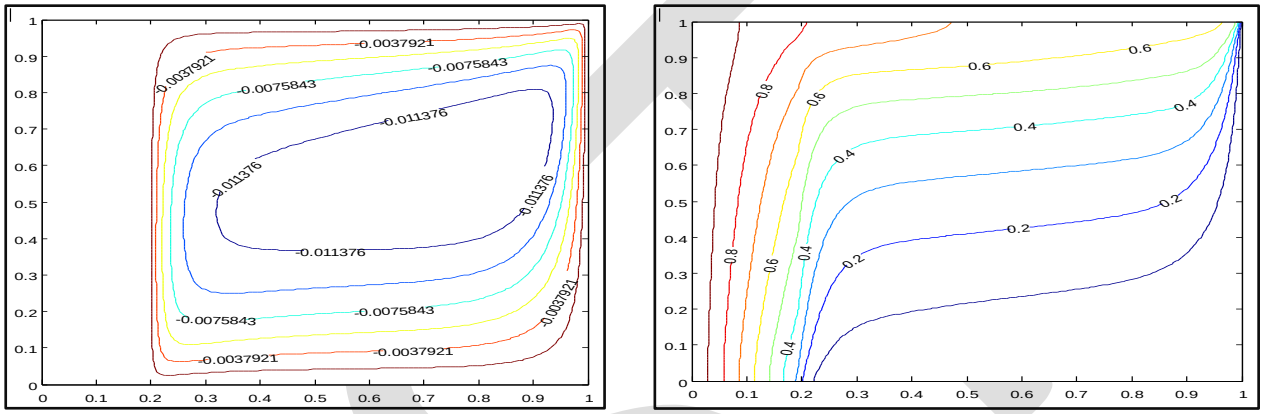

(b)|Ψ|=0.013272

Fig 1. Comparison of Streamlines (Left) and Isotherms (Right) at Ra=1000,kr=2.4,D=0.2
(a) numerical results of Saleh (2012), (b) present study

Table 1. Comparison of $(\overline{Nu})_p$ values with some results from the literature for Kr = 1 and Ra=1000

D	Saeid (2007)	Saleh(2012)	Present study
0.1	5.044	4.926	5.269
0.2	3.186	3.094	3.250
0.5	1.566	1.532	1.568

4. RESULTS AND DISCUSSION

The analyses in the undergoing numerical investigation are performed in the following domain of the associated dimensionless groups: the ratio of wall thickness to its height ($0.25 \leq D \leq 0.375$); the wall to porous thermal conductivity ratio ($0.1 \leq Kr \leq 10$); the porosity ($0.2 \leq \epsilon \leq 0.9$); the Darcy number ($10^{-6} \leq Da \leq 1$); and the Rayleigh number ($10^3 \leq Ra \leq 10^6$). The results are presented as streamlines and streamlines. The rate of heat transfer in the enclosure is measured in terms of the average Nusselt number.

4.1 Effects of Rayleigh number(Ra) and the wall to porous thermal conductivity ratio(kr):

The effects of the variation of Rayleigh number (Ra) on the isotherms and streamlines for different values of thermal conductivity ratio (kr) are shown in Figure 5 and Figure 6. At all values of (Ra) and (kr=0.1), the isothermal lines seem to be a vertical parallel lines which are very close to pure conduction, as (kr) increases a gradual increasing development of convective motion is occur the isothermal lines seem to be a vertical parallel lines which is very close to pure convection when comparing two consecutive state. Increasing of thermal Rayleigh number decreased the heat transfer rate and therefore leading to decrease the average Nusselt number for all values of (kr). The same figures show effect of thermal conductivity ratio (k_w/k_p) on heat transfer rate. These figures illustrates that the average Nusselt number is increasing with increase of thermal conductivity ratio, also the most of the temperature variation still in the wall thickness with lower (kr) and gradually transfer into the porous media with increase of values of (kr), and from streamlines we note that increasing ($|\Psi_{max}|$) with increasing of (kr). It is also observed that convection effects inside the porous medium become stronger for higher values of (kr).

4.2 Effects of wall thickness (D):

To show the effects of the wall thickness (D=d/H), streamlines and isotherms are presented in Figure 7 for (Ra=1000, kr=1, $Da=10^{-6}$, $\epsilon = 10^9$ and Pr=1). The isotherms lines are vertical parallel in all cases of (D) and the average Nusselt number increases when the wall thickness(D) increases, this means the heat transfer convection is dominant in the porous enclosure. The strength of the flow circulation of the fluid-saturated porous medium is much higher for a thin wall, and the value of $|\Psi_{max}|$ decreases as (D) increases. Fig.7 displays the variation of the average Nusselt number along the interface with (D) for different (Kr). For lower value of kr (kr=0.1), the average Nusselt number decreases with increases of (D), and it becomes approximately constant when ($k_w = k_p$), i.e. (kr=1), for the higher value of kr (kr=10), the relation becomes proportionally, i.e. $\left(\text{D increase} \rightarrow (\overline{Nu})_p \text{ increase}\right)$. This indicates the effect of the conduction heat transfer on the natural convection through the porous enclosure.

4.3 Effects of porosity (ϵ):

Figure 8 illustrates the effects of the porosity (ϵ) on the thermal fields and the circulation of the fluid in the porous enclosure, the isotherms and streamlines are presented for (Ra=1000, kr=1, D=0.25,$Da=10^{-6}$, and Pr=1). It is clear from this figure that increase of porosity led to farther distortion of isothermal lines which mean increase of convection heat transfer due to increase of the amount of fluid in motion. The increase of porosity led to decrease in fluid velocity because the passages between the solid particles become larger as void ratio is increase. This can be noted from streamlines patterns which decrease in strength with porosity increase. As resultant, the $(\overline{Nu})$ increases and ($|\Psi_{max}|$) decrease as porosity values increase.

4.4 Effects of Darcy number (Da):

Figure 3 shows the average Nusselt number for different thermal conductivity ratio (kr) with different Darcy number. We note meager different between Darcy values and average Nusselt numbers as (kr=0.1) and clear variation in values of $(\overline{Nu})$ as (kr=1,10), we can see as (kr=0.1,1,10) and ($10^{-6} \leq Da \leq 10^{-3}$) the values of $(\overline{Nu})$ decrease, but as ($10^{-3} \leq Da \leq 1$) and (kr=1,10) the values of $(\overline{Nu})$ increase, but as (kr=0.1) we show

there is an instability in values of $(\overline{Nu})$, that is meaning the effect of Darcy number it seems to be clear with values of (kr ≥1), i.e. as $(k_p \geq k_s)$.

4.5 Variation of $(\overline{Nu})$ with (Ra) for difference value of (D):

The variation of the average Nusselt number with the Rayleigh number is shown in Figure 4 for different values of (D). Figure 4 shows that reducing the solid wall thickness leads to the enhancement in the heat transfer by natural convection and increase the average Nusselt number for (kr=1). the unusual behavior is observed at high values of $(6 * 10^4 \leq Ra \leq 10^5)$ where it is found that $(\overline{Nu})$ is reducing with reducing of the wall thickness(D). This means that the thermal resistance of the wall is less than that of the porous medium.

5. CONCLUSION

In this article, we have studied numerically the effects of a conductive wall on natural convection heat transfer in a rectangular enclosure filled with porous media sandwiched by two finite thickness walls. the Brinkman-Forchheimer-extended Darcy mode is used in the mathematical formulation for the porous layer. The governing parameters considered are the Rayleigh number $(10^3 \leq Ra \leq 10^6)$, the wall to porous thermal conductivity ratio $(0.1 \leq Kr \leq 10)$, the Darcy number ($10^{-6} \leq Da \leq 1$), the porosity of the porous region $(0.2 \leq \epsilon \leq 0.9)$, and the ratio of wall thickness to its height $(0.25 \leq D \leq 0.375)$. The non-dimensional forms of the continuity, momentum and energy equations are solved numerically by using the (ADI with Relaxation parameter) method in the uniform grid in both horizontal and vertical directions. It is found that the increasing of thermal Rayleigh number (Ra) decreased the heat transfer rate and therefore leading to decrease the average Nusselt number for all values of (kr), also the average Nusselt number and $(|\Psi_{max}|)$ are increasing with increase of thermal conductivity ratio (kr). The isotherms lines are vertical parallel in all cases of (D) and the average Nusselt number increases when the wall thickness(D) increases, this means the heat transfer convection is dominant in the porous enclosure. The increase of porosity led to farther distortion of isothermal lines which mean increase of convection heat transfer due to increase of the amount of fluid in motion and streamlines patterns decrease in strength with porosity increase. As resultant, the $(\overline{Nu})$ increases and $(|\Psi_{max}|)$ decrease as porosity values increase. We note meager different between Darcy values and average Nusselt numbers as (kr=0.1) and clear variation in values of $(\overline{Nu})$ as (kr=1,10), as (kr=0.1,1,10) and $(10^{-6} \leq Da \leq 10^{-3})$ the values of $(\overline{Nu})$ decrease, but as $(10^{-3} \leq Da \leq 1)$ and (kr=1,10) the values of $(\overline{Nu})$ increase. Reducing the solid wall thickness leads to the enhancement in the heat transfer by natural convection and increase the average Nusselt number for (kr=1).). This means that the thermal resistance of the wall is less than that of the porous medium.

REFERENCE

[1] A. Al-Amiri, Khanafer and K., Pop, I.: Steady-state conjugate natural convection in a fluid-saturated porous cavity. Int. J. Heat Mass Transf. 51, 4260–4275, (2008).

[2] D.A. Nield and A. Bejan, Convection in Porous Media, third ed., Springer, New York, 2006.

[3] D.B. Ingham and I. Pop (Eds.), Transport Phenomena in Porous Media, Elsevier, Oxford, 2005..

[4] G. Lauriat, and V. Prasad, Non-Darcian effects on natural convection in a vertical porous enclosure, Int. J. Heat Mass Transfer 32 (1989) 2135–2148, (1989).

[5] H. Saleh and L. Hashim Conjugate natural convection in a porous enclosure with non-uniform heat generation, Transp Porous Med 94:759-774, (2012).

[6] H. Saleh, N.H. Saeid, Hashim, and I., Mustafa, Z.: Effect of conduction in bottom wall on Darcy-Bénard convection in a porous enclosure. Transp. Porous Media 88, 357–368 (2011).

[7] K. Vafai (Ed.), Handbook of Porous Media, second ed., Taylor & Francis, New York, (2005).

[8] K. Vafai and H. Hadim, Overview of current computational studies of heat transfer in porous media and their applications – natural and mixed convection, in:W.J. Minkowycz, E.M. Sparrow (Eds.), Advances in Numerical Heat Transfer, vol. II, Taylor & Francis, New York, (2000). Chapter 10.

[9] P. Vadasz (Ed.), Emerging Topics in Heat and Mass Transfer in Porous Media, Springer, New York, (2008).

[10] Y. Varol, H.F. Oztop, M. Mobedi and Pop, I.:Visualization of heat flow using Bejan'sheatline due to natural convection of water near 4◦C in thick walled porous cavity. Int. J. Heat Mass Transf. 53, 1691–1698 (2010).

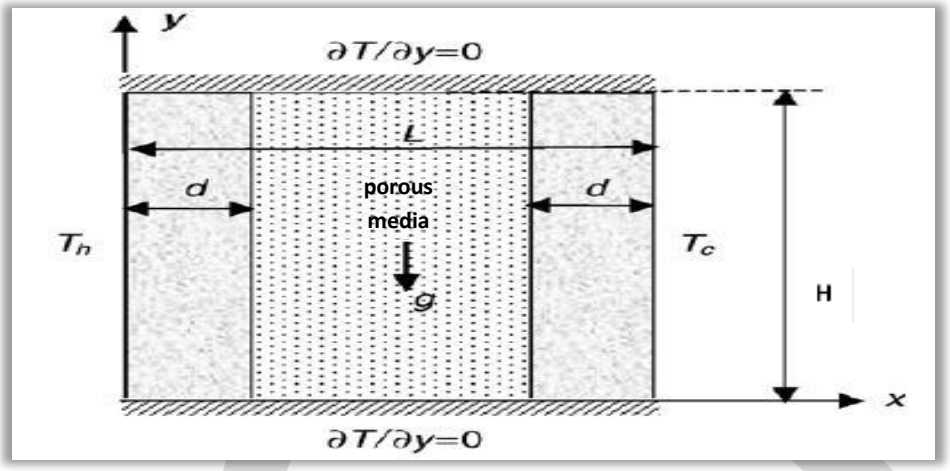

Fig 2. Schematic Diagram of The Physical Model and Coordinate System

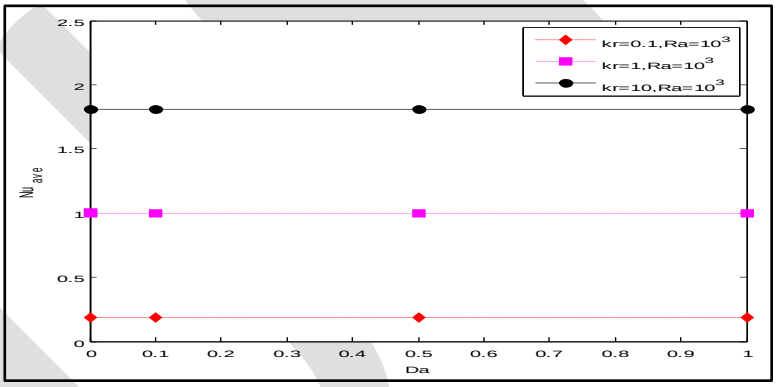

Fig 3. Variation of The Average Nusselt Number Along The Interface With Da for Different Kr

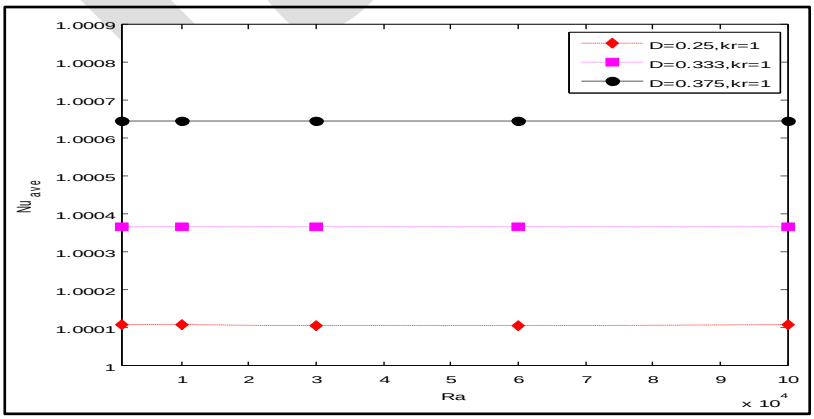

Fig 4. Variation of The Average Nusselt Number Along The Interface With Ra for Different D

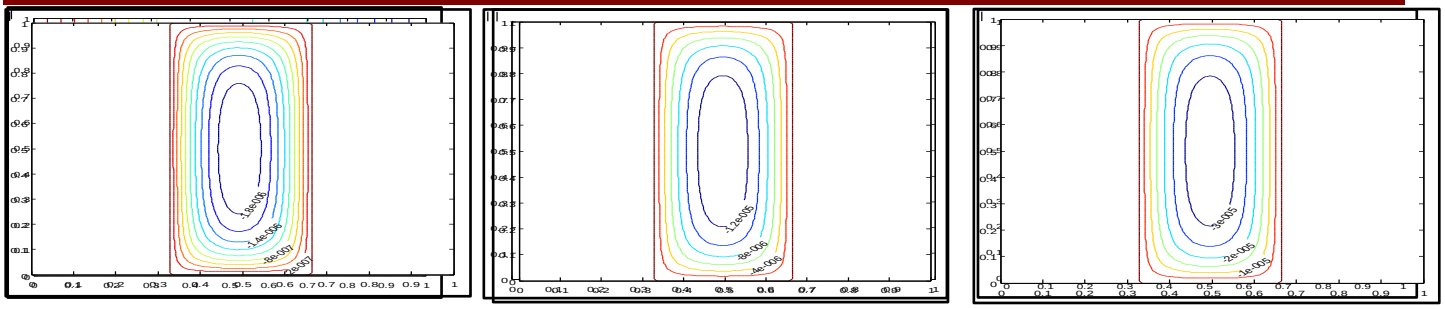

[1]: (a)) $\overline{Nu}$= 0.143388341811744 (b)$\overline{Nu}$=1.00036805122612 (c)$\overline{Nu}$= 2.479774590862095

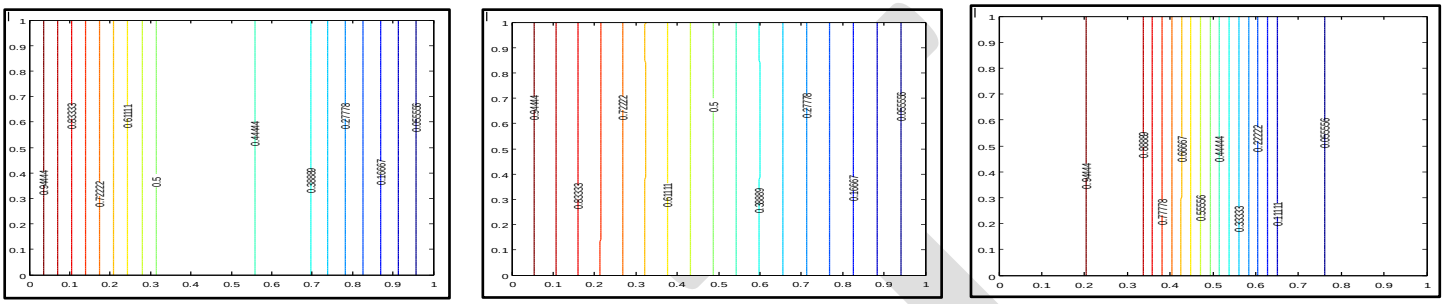

[2]: (a) $\overline{Nu}$=0.143388340773647 (b)$\overline{Nu}$=1.000367862338257 (c)$\overline{Nu}$= 2.479772945968539

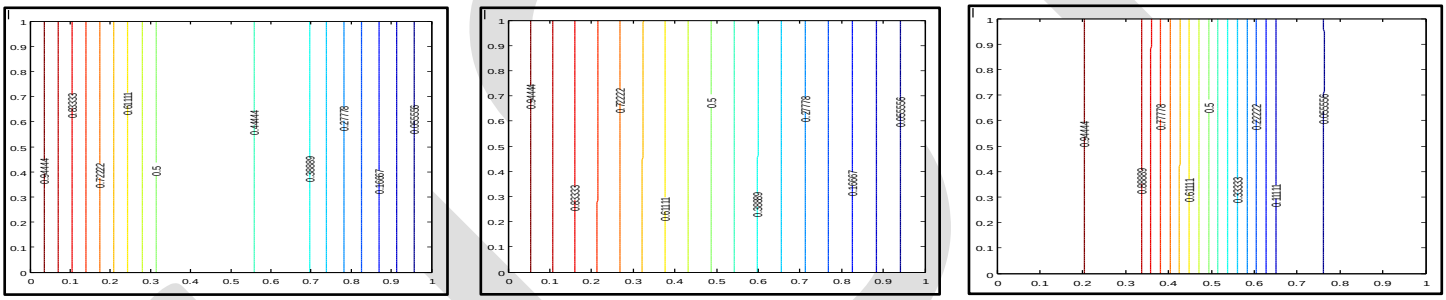

[3]: (a)$\overline{Nu}$= 0.143388330455602 (b)$\overline{Nu}$=1.000366041953630 (c)$\overline{Nu}$= 2.479757664432117

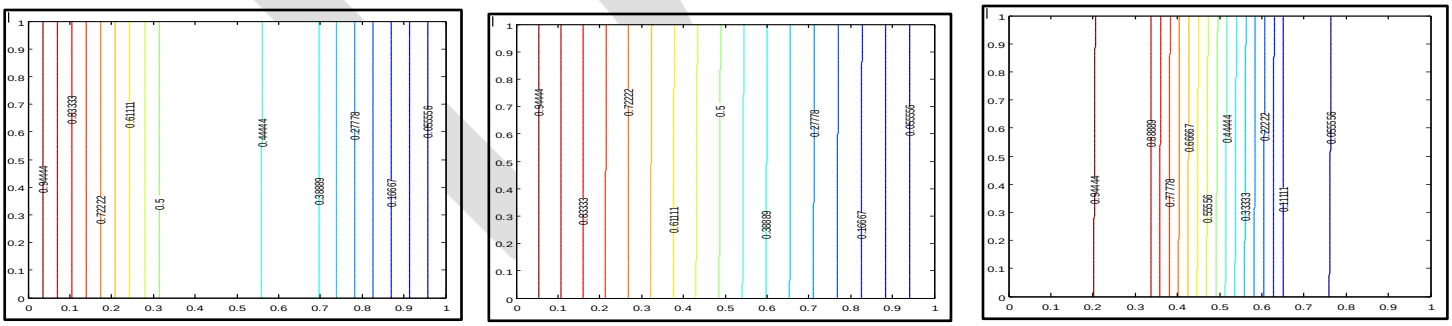

[4]: (a)$\overline{Nu}$= 0.143388233566735 (b)$\overline{Nu}$=1.000354687568599 (c)$\overline{Nu}$= 2.479721573919110

Fig 5. Isotherms for H=L , L1/L2=1: (a) kr=0.1,(b) kr=1, (c) kr=10 for: [1] Ra=1000, [2] Ra=10000, [3] Ra=100 000, [4] Ra=1000 000

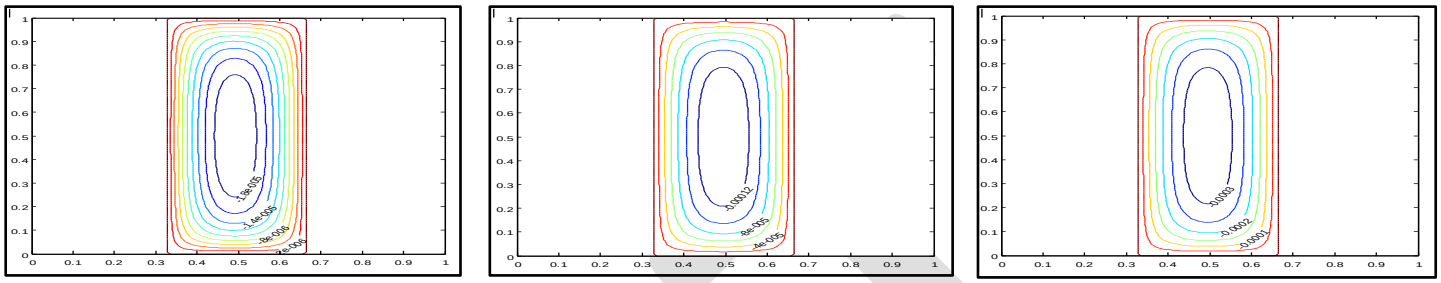

[1]:(a)$|\Psi_{max}|$=1.981897380554446e-6 (b)$|\Psi_{max}|$=1.381720115623780e-5 (c)$|\Psi_{max}|$=3.409366052518965e-5

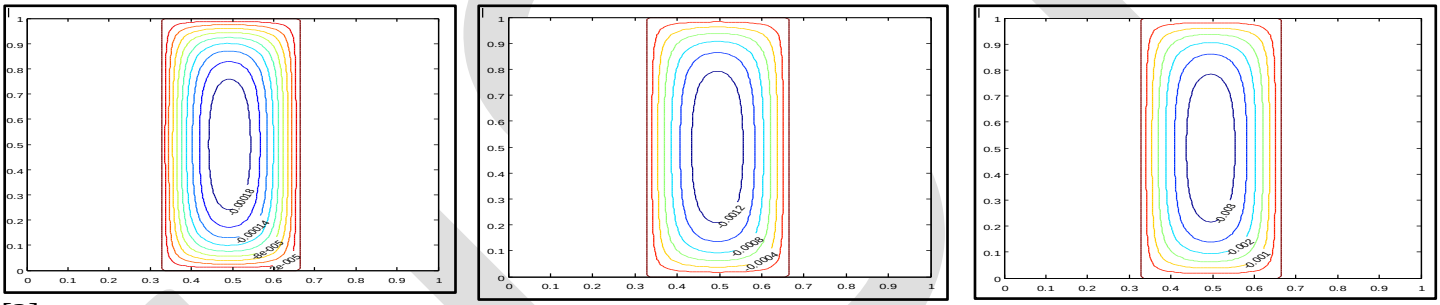

[2]:
(a)$|\Psi_{max}|$=1.9818973584764e5 (b)1.381719998375207e-4 (c)$|\Psi_{max}|$=3.409365380247637e-4

[3]:(a)$|\Psi_{max}|$=1.981897111542511e-004 (b)$|\Psi_{max}|$=0.001381718568537 (c)$|\Psi_{max}|$=0.003409358190789

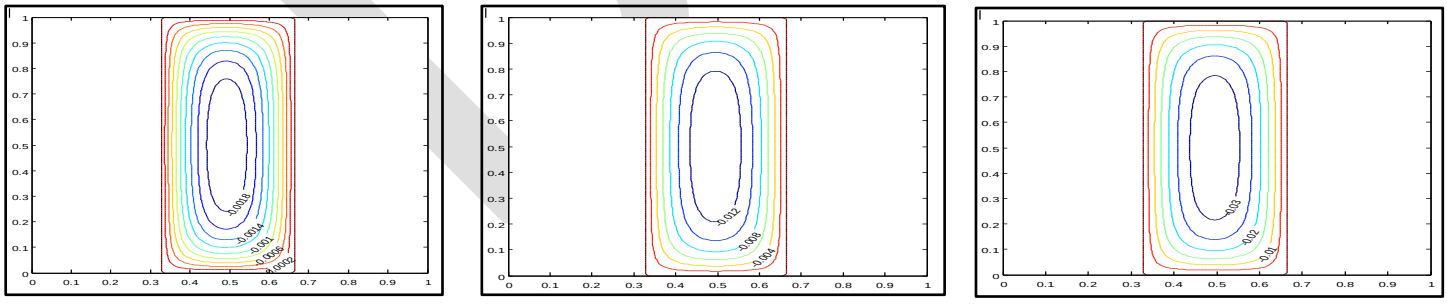

[4]:(a)$|\Psi_{max}|$=0.001981892026906 (b)$|\Psi_{max}|$=0.013816788677204 (c)$|\Psi_{max}|$=0.034092396279920

Fig 6. Streamlines for H=L , L1/L2=1: (a) kr=0.1,(b) kr=1, (c) kr=10 for:[1] Ra=1000, [2] Ra=10 000, [3] Ra=100 000, [4] Ra=1000 000

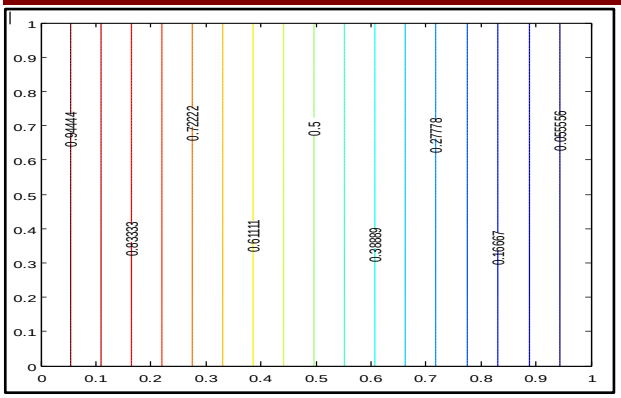

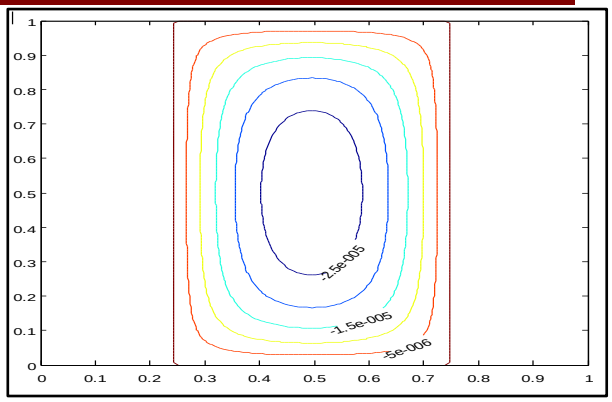

$\overline{Nu}$=1.000109032478825 (a): D=0.25 $|\Psi_{max}|$=2.882374247793044e-005

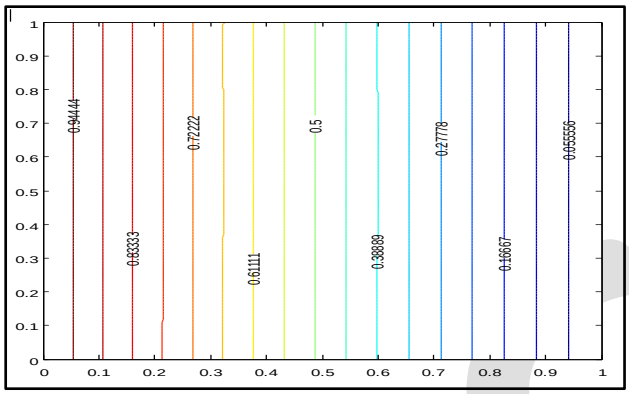

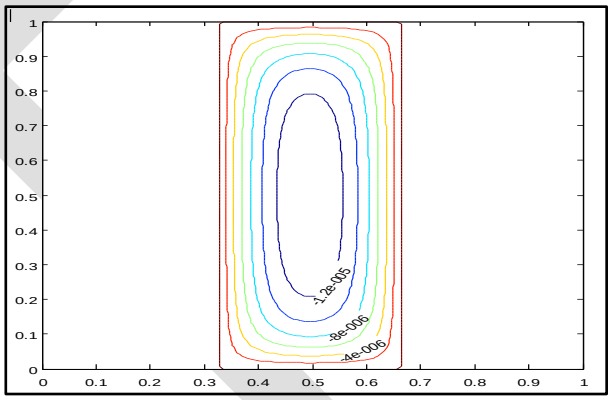

$\overline{Nu}$= 1.000368051226120 (b): D=0.333 $|\Psi_{max}|$=1.381720115623780e-005

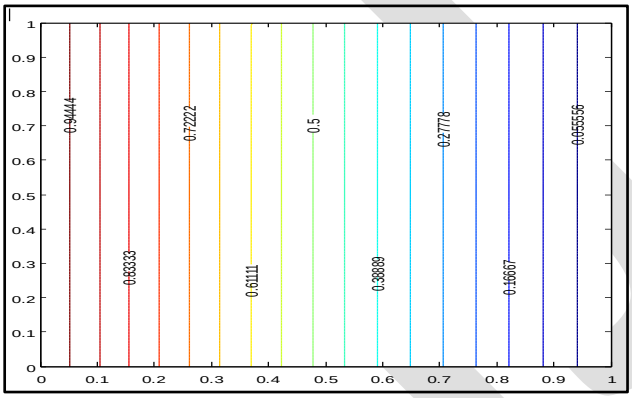

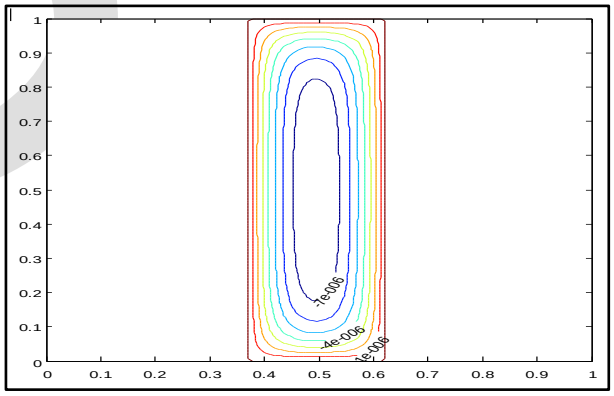

$\overline{Nu}$= 1.000646592584926 (c): D=0.375 $|\Psi_{max}|$=7.886965665065630e-006

Fig 7. Isotherms (Left), Streamlines (Right) at Ra = 1000, Kr = 1 for Different Values of D

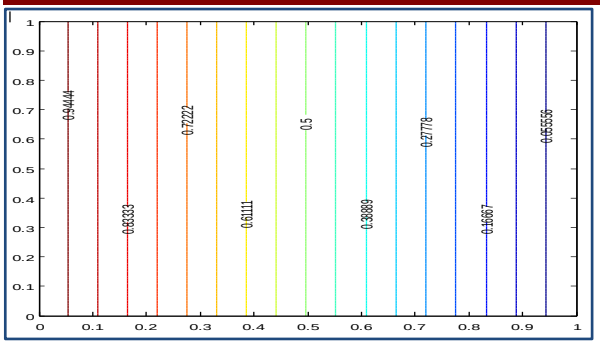

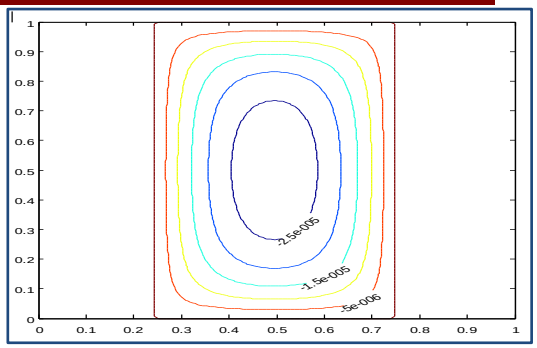

$\overline{Nu}$=1.000070195238852 (a): porosity=0.2 $|\Psi_{max}|$=2.865324364595038e-005

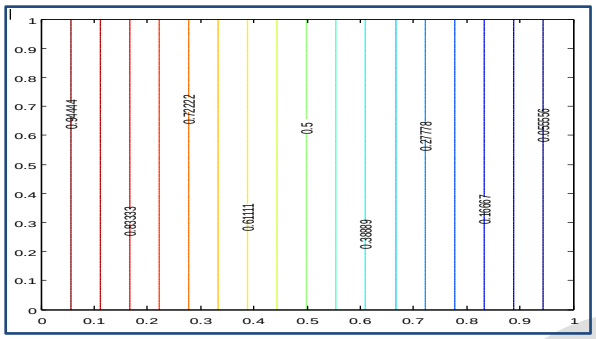

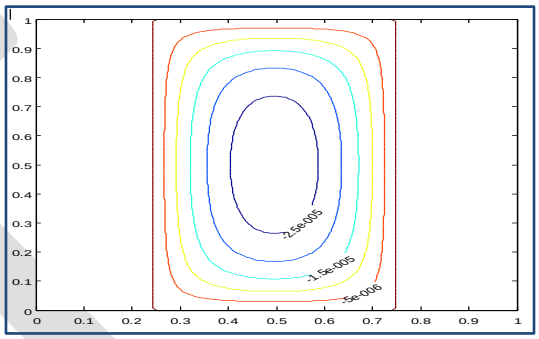

$\overline{Nu}$=1.000021655859216 (b): porosity=0.4 $|\Psi_{max}|$=2.875441650122583e-005

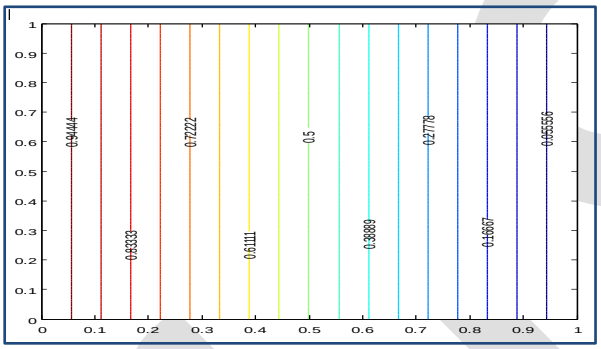

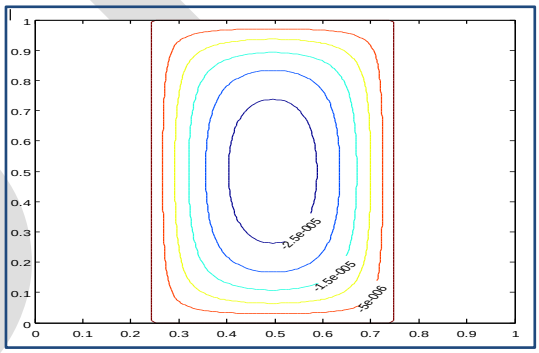

$\overline{Nu}$=1.000000805187454 (c): porosity=0.6 $|\Psi_{max}|$=2.879052932709430e-005

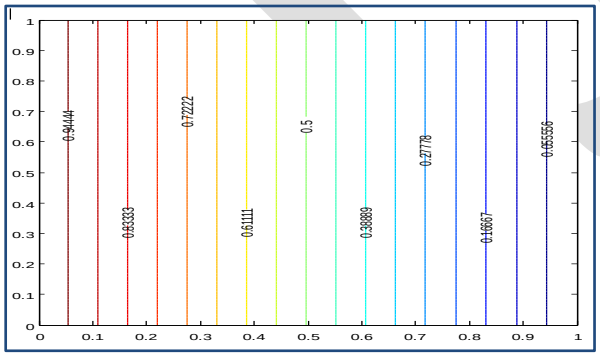

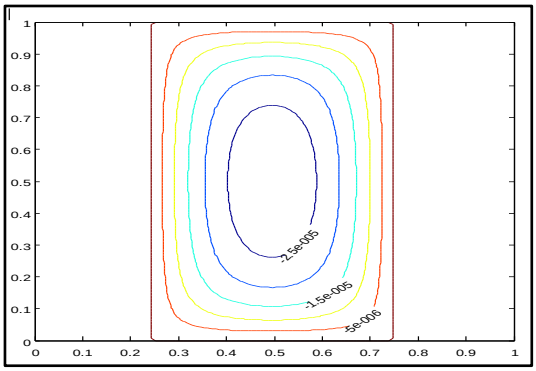

$\overline{Nu}$=1.000109032478825 (d):porosity=0.9 $|\Psi_{max}|$=2.882374247793044e-005

Fig 8. Isotherms (Left), Streamlines (Right) at Ra = 1000, Kr = 1 for Different Values of Porosity